Modelling and control of a Fuel Cell System and its Storage Elements in transport applications

Stéphane Caux, Jérôme Lachaize, Maurice Fadel, Pascal Schott, Laurent Nicod

MODELLING AND CONTROL OF A FUEL CELL SYSTEM AND ITS STORAGE ELEMENTS IN TRANSPORT APPLICATIONS

S.Caux*[1], J.Lachaize[1], M.Fadel[1],P.Shott[2], L.Nicod[3]

1-Laboratoire d'Electrotechnique et d'électronique industrielle, LEEI INPT, UMR, CNRS- 2 rue Camichel - 31071 Toulouse cedex 7-France.
Tel : +33(0)5 61 58 82 08
lachaize@leei.enseeiht.fr ;fadel@leei.enseeiht.fr ; caux@leei.enseeiht.fr
2-Laboratoire Hydrogène et Pile à Combustible, CEA/LITEN/DSEN/SGPAC/LPAC -*17 rue des Martyrs – 38054 Grenoble cedex 9 France.*
Tel: +33(0)4 38 78 48 40
pascal.schott@cea.fr
3-ALSTOM Transport SA, rue du docteur guinier BP 4- 65600 Séméac – France.
Tel : +33(0)5 62 53 48 57
laurent.nicod@transport.alstom.com

Abstract: This paper presents in a first step, a modelling approach to control auxiliaries of a PEM Fuel Cell and the design of control laws. Anode and Cathode compartments are considered to derives the voltage behaviour of the Fuel Cell and to control air and hydrogen flow rate as well as pressure. In a second step, the structure specification of an electrical power train with Fuel Cell for high power transport applications is presented. Two choppers are designed and controlled to deliver the power demand from the Fuel Cell itself and Storage Elements added. This work shows that we can characterise and adjust the system control on an actual operating cycle.

Keywords : PEMFC Modelling, Power Control

1- Introduction

The use of Fuel Cells is now envisaged to supply electrical energy in high power rail transport applications. Mainly due to pollution regulations there is a growing interest in using non conventional energy in transport applications and over the last decade Fuel Cell Systems have shown considerable promises [1],[2]. Alstom-Transport has commenced a project to build a high power electrical train using PEM Fuel Cell and Energy Storage Elements to feed its engines. The collaboration with the CEA (French Atomic Energy Centre) has allowed us to establish and work with an accurate electro-chemical model of the Fuel Cell behaviour. In this paper a complete study of the control of the entire electrical power train, including the Fuel Cell sub-system, actuators and the chopper, is conducted. Actual load demands from existing traction applications are used in the simulation and the ability to track these load demands is investigated, as well as the specific regulation of the sub-sytems (i.e. Fuel Cell, chopper, etc.). This works presents modelling method and control approach of non-conventional energy sources and distributed power generation.

In a first time, we present the Fuel Cell model and its auxiliaries used to design the Fuel Cell controllers. Then we explain the control strategy of these auxiliaries, only for air flow compressor and air valve pressure.

*[1] corresponding author : Caux stéphane : E-mail : caux@leei.enseeiht.fr Tel: +33 5 61 58 82 51 Fax: +33 5 61 63 88 75

In a second time, we detail the power train structure and the control scheme of each electrical chopper. Finally first result of energy management are shown not only to validate the accurate tracking of power demand but also to verify the correct management of the Fuel Cell System (voltage control) and charge and discharge of the Storage Elements.

2- Fuel Cell System.

The Fuel Cell System is composed by the fuel cell core associated with all the necessary auxiliaries for an embedded fuel cell system. The Figure 1 represents all the functions present in a Fuel Cell System.

The modelling process consists in writing the variations of the species concentrations, then in calculating the pressure in each compartment. After this step we use a quasi-static model to establish the voltage variation of the Fuel Cell [1] [2].

The demanded power needed in our high power electric train application can not be supplied by one based-cell. Therefore to obtain the 440 kW nominal power and 375 V at the Fuel Cell's terminal (1173 A output), we use a Fuel Cell Stack made with 586 based-cells. This stack can be modelled by a single Fuel Cell with an effective membrane surface area of 1956 cm^2, allowing us to treat only one air and one hydrogen source. The Fuel Cell Stack and auxiliaries (i.e. compressor, valves, etc.) are called the Fuel Cell System (FCS).

The DC bus is designed to be 750V and the Fuel Cell does not allow bi-directional current flow. Therefore Energy Storage Elements are provided (typically 7 parallel stacks of 304 supercaps), to absorb or deliver energy depending on the load profile (demanded load power). Given the properties of the Fuel Cell and the value of the DC bus, the operation of the two chopper circuits is determined (i.e. chopper 1 is a boost allowing uni-directional power flow, chopper 2 is a buck/boost circuit with bi-directional power flow). There are different kinds of Fuel Cells depending on the operating temperatures at which they work and technology used for the electrolytic separation [3],[4]. In our application we use a Proton Exchange Membrane (PEM) Fuel Cell which is becoming more attractive for mid-power applications and seems to be well suited for embedded systems. This choice determines some important parameters which must be regulated to a constant value. This can be achieved either by physical construction (eg. Pipe geometry, membrane area) or through control action (eg; flow rate, pressure).

In this study, we work at low-pressure and mid-temperatures :

- Temperature : 80°C $T_{fc} = 353.15°K$
- Air Pressure : 1.5 bars $P_{outlet} = 1\ 10^5 Pa$; $P_{inlet} = 1.5\ 10^5 Pa$
- Hydrogen Pressure : P_{H2}=2 bars

The nominal point of the system is:

$StO_2 = 1.6$; $Power\_nom = 400kW$; $Unom_{\min} = 375V$

3- Fuel Cell Modelling.

3.1- Cathodic species schedule.

The following equations describe the variations of the gaseous species concentrations in the cathode compartment (see appendix). The balance of oxygen and nitrogen allows us to write :

$$\begin{cases} \frac{dnO_2}{dt} = 0.21F_{in} - F_{O_2c} - X_{0_2}F_{valve} \\ \frac{dnN_2}{dt} = 0.79F_{in} - X_{N_2}F_{valve} \\ \frac{dn_{vap}}{dt} = \frac{X_{vap}}{1-X_{vap}}F_{in} - X_{vap}F_{valve} \end{cases} \quad (1)$$

Where: $F_{O_2c} = \frac{NI_{fc}}{4F}$ $X_{vap} = \frac{P_{sat}(T_{fc}°)}{P_{cath}}$ $X_i = \frac{P_i}{P_{cath}}$

With :

- *Fin* inlet molar flow of the compressor.
- *Fvalve* outlet molar flow of the valve.
- *Xi* molar fraction of i species .
- FO_2c oxygen molar flow consumed by the fuel cell.

3.2- Anodic species schedule.

In the anodic compartment, we can write the same type of balance.

$$\frac{dnH_2}{dt} = F_{H_2in} - F_{H_2c} - F_{H_2valve} \qquad F_{H_2c} = \frac{NI_{fc}}{2F} \quad (2)$$

With :

- F_{H2in} inlet molar flow of the Reducing valve.
- F_{H2c} hydrogen molar flow consumed by the Fuel Cell.
- $F_{H2valve}$ outlet molar flow of the valve due to periodic purge made.

3.3- Pressure calculation.

Knowing the concentration species, we use the perfect gas law assumptions to calculate the pressure:

$$P_{cath} = \frac{RT_{fc}}{V_{cath}}(n_{O_2} + n_{H_2} + n_{vap}) \quad (3)$$

The dynamic model of the pressure variation is:

$$P_{cath} = \frac{RT_{fc}}{V_{cath}}\frac{1}{p}\left((1+\frac{X_{vap}(P_{cath},T_{fc})}{1-X_{vap}(P_{cath},T_{fc})})F_{comp} - F_d\right) \quad (4)$$

With: $F_d = F_{O2_{cons}} + F_{valve}$ a new variable containing F_{O2c} a disturbance which will be rejected after by the controller.

We can also calculate the partial pressures:

$$P_{O_2} = \frac{RT_{fc}}{V_{cath}} n_{O_2} \qquad P_{H_2} = \frac{RT_{fc}}{V_{cath}} n_{H_2} \qquad (5)$$

3.4- Voltage calculation.

The voltage variation of the Fuel Cell are calculated with a quasi-static model, because the chemical reaction dynamic is faster than the system dynamics. This voltage depends on the current density in the Fuel Cell, the partial pressures (of hydrogen and oxygen), the temperature of the reaction, and the hydration of the membrane so :

$Ufc = f(I, PO_2, PH_2, T_{fc}°, \lambda_{H_2 0})$

Assumptions for the model :

- Insignificant Anodic activation voltage.
- Uniform current density.
- Uniform temperature.

The voltage expression is:

$$Ufc = E_{Nernst} - \frac{RT_{fc}}{2\alpha F} \ln\left(\frac{j}{j_o}\right) - R_{mem}\, j - j\left(c\frac{j}{j_{\max}}\right)^2 \quad (6)$$

With :

- α= symmetry factor (0,5).
- j_o = current exchange.j_0=[10^{-7}A/cm^2;10^{-5}A/cm^2].
- R_{mem}=f(T_{fc},λ_{H2O}) membrane resistance (0,162 Ω/cm^2).
- j_{max}=2.5A/cm^2 maximum current.
- c=0.471 coefficient due to simplification.

In the voltage curve obtained in Figure 2, we can see three zones:

- Cathodic activation (zone one) : $\frac{RT_{fc}}{2\alpha F} \ln\left(\frac{j}{j_o}\right)$.
- Ohmic loss (zone two) :$R_{mem}\, j$.
- Diffusion limitation (zone three) : $j(c\, j / j_{\max})^2$.

The Nernst law is valid on all the voltage range. This law represents the voltage of the oxidation-reduction reaction :

$$E_{Nernst} = \frac{\Delta G^0}{2F} + \frac{RT_{fc}}{2F} \ln\left(\sqrt{\frac{P_{O_2}}{10^5}} \frac{P_{H_2}}{10^5}\right)$$

4- Compressor Modelling.

After Modelling the PEM core, we must study the air supply process to obtain the dynamics of the voltage developed by the Fuel Cell.

For the Fuel Cell to deliver the demanded power at the desired output voltage, the air circuit must supply the Fuel Cell with a sufficient flow rate of air at a target air pressure of 1.5 bars. In a state space sense, the air pressure and flow rate in this circuit are coupled, but it is possible to decouple the control of these two parameters in the following fashion. The air circuit makes use of a compressor and a valve, providing two control parameters – the speed of the synchronous machine that drives the compressor (used to regulate flow), and the set point of the valve (used to regulate pressure). In this next section the mathematical modelling of this loop is presented. This includes the linearisation of the compressor components in the system and then, the design of decoupled controllers for both the pressure and flow within the loop. The air supply system of the Fuel Cell is composed by a screw type compressor. We choose this type of compressor to avoid the flow oscillations and the lubrication. The rotation is made by a synchronous drives with permanent magnets.

Remark : we work here on a low-pressure Fuel Cell System.

4.1- Outlet flow compressor.

The outlet flow is detailed in [3] and is:

$$q_{molar} = \frac{P_{outlet}}{RT_{outlet}} Cyl \frac{\omega}{2\pi} \eta_v \qquad (7)$$

The volumetric efficiency η_v allows us to include several phenomena in the model :

- The total mechanical clearances between rotor and compressor casing .
- Compression rate.
- Rotor peripheral speed.
- Flow density.

The volumetric efficiency depends on the rotor speed and compressor rate ($tx = \frac{P_{outlet}}{P_{inlet}}$) as seen in Figure 3.

4.2- Flow simplification modelling.

The association of the synchronous machine (with speed control) and the compressor can be represented by the diagram presented in Figure 4. From this functional diagram we can build a structure, to write the evolution law of the compressing flow. The solution used in this study involves passing the flow reference (F_{lin}) through the a look-up table that contains the inverse characteristic of the compressor, to produce the required speed reference. Note that this table is a function of pressure as well as flow. The inverse model is representing by the Figure 5 maps contained in a look-up table in Matlab. Therefore, we can write the diagram in Figure 6.

The synchronous engine and its controller are equivalent to a first order system. So the exit flow of the compressor is represented by:

$$F_{comp} = \frac{1}{p}\left(\frac{1}{\tau} F_{lin} - \frac{1}{\tau} F_{comp}\right) \qquad (8)$$

5- Valves Modelling.

The molar flow of the valves is expressed in function of the opening section, the temperature, and the outlet and inlet pressures [4]:

$$F_{valve} = S_{open}\sqrt{\frac{2P_{inlet}^{\ 2}}{MRT_{inlet}}\frac{\gamma}{\gamma-1}\left(\frac{P_{outlet}}{P_{inlet}}\right)^{\frac{2}{\gamma}} - \left(\frac{P_{outlet}}{P_{inlet}}\right)^{\frac{\gamma+1}{\gamma}}} \qquad (9)$$

This valve models is linearised around the nominal point: So the new model is only a gain function :

$$F_{valve} = S_{open} K_{valve}$$

6- Auxiliary control strategy

6.1- Steady state modelling.

The model of the Fuel Cell air-system results in a model with two states [2][5], where:

$$X = [\text{Pcath Fcomp}]^t$$

$$\dot{X} = \begin{bmatrix} 0 & (1+\frac{X_{vap}(P_{cath},T_{fc})}{1-X_{vap}(P_{cath},T_{fc})})\frac{RT_{fc}10^{-5}}{V_{cath}} \\ 0 & -\frac{1}{\tau} \end{bmatrix} X + \begin{bmatrix} -\frac{RT_{fc}10^{-5}}{V_{cath}} & 0 \\ 0 & -\frac{1}{\tau} \end{bmatrix} \begin{bmatrix} Fd \\ F_{lin} \end{bmatrix}$$

Remark : in this model the pressure is in bar (coefficient 10^{-5}).

The non-linear model is linearised around the nominal point. So we can write :

$$\dot{X} = \begin{bmatrix} 0 & (1+\frac{X_{vap_n}}{1-X_{vap_n}})\frac{RT_n10^{-5}}{V_{cath}} \\ 0 & -\frac{1}{\tau} \end{bmatrix} X + \begin{bmatrix} -\frac{RT_n10^{-5}}{V_{cath}} & 0 \\ 0 & -\frac{1}{\tau} \end{bmatrix} \begin{bmatrix} Fd \\ F_{lin} \end{bmatrix} \qquad (10)$$

6.2- Feedback Control Design.

Digital system controllers are implemented, so the state model must be discretised. The sampling frequency selected is equal to : $fe = 100Hz$

The new state model is:

$$X(k+1) = A_d X(k+1) + B_d u(k) \text{ and } Y(k) = C_d X(k)$$

In order to decouple the two state variables, a controller of the form shown in Figure 7 is used with the control law as :

$$u(k) = \Delta^{-1} v(k) - \Delta^{-1}\Delta_0 X(k) \qquad (11)$$

With: $\Delta = B_d$ and $\Delta_0 = A_d$

With this state feedback controller the resulting system is simplified and the plant model is equivalent to introducing a transport delay for each new state obtained (v_1, v_2), according to :

$$P_{cath} = z^{-1}v_1 \text{ and } F_{comp} = z^{-1}v_2 .$$

After decoupling the system we implement RST regulator in order to control the two variables with different dynamic.

The regulator structure is shown on Figure 8.

Where:

$$S(z^{-1}) = 1 - z^{-1}; R(z^{-1}) = r_0 + r_1 z^{-1} \; T = R(1) \qquad (12)$$

The polynomial regulator coefficients are calculated by the pole placement. The characteristic polynomial of the closed loop becomes :

$$P(z^{-1}) = 1 + p_1 z^{-1} + p_2 \; z^{-2} = (1 - z^{-1} \exp(-\omega Td))^2 \qquad (13)$$

with:

$\omega = 15\, rad/s$ for pressure loop.

$\omega = 50\, rad/s$ for flow compressor loop.

We obtain:

$$r_0 = p_1 + 1 \; and \; r_1 = p_2 \qquad (14)$$

Pressure reference *Pref*=15bar. The flow reference is calculate with the Faradays law:

$$F_{ref} = \frac{N\, I\, St_{O2}}{4F\, X_{0_2}} \qquad (15)$$

6.3- Simulation results.

The results of simulation in Figure 9 and 10, represents the evolution of pressure and flow when power is requested on Fuel Cell. It is realised with the very complete model on Matlab/Simulink.

As we can see on this simulation the pressure is remained constant despite the compressor flow variation. We can also see that the compressor flow tracks the flow reference.

7- Traction chain.

7.1- Architecture.

The Fuel Cell is now connected to the DC link with an electronic chopper (CVS1-Boost Chopper). The existing Fuel Cell sub-system has to be designed for high power and does not exist for the moment. That is why an Energy Storage System (ESS) must be associated with the Fuel Cell. In addition the ESS is able to absorb the braking energy of the vehicle. The ESS technology chosen is supercaps. This ESS is connected to the DC link by another electronic chopper (CVS2-full Chopper). The source and storage elements must contribute to achieve the demanded power, used to supply the traction and auxiliary loads (eg. Lighting, air conditioning, etc.) of the vehicle. The electrical choppers are shunt connected as shown on Figure 11.

In transport applications the voltage of the DC link is high. Chopper CVS1 is controlled for the DC link voltage regulation. So a loop voltage regulation is used.

The supercaps chopper (CVS2) is a Buck/Boost because this chopper must be bi-directionnal in current. This chopper control is a current regulation to manage the charge and discharge of the ESS. The current reference is calculated in function of the ESS power reference that is obtained by an energy strategy.

7.2- Boost Modelling and Control

The power switch is controlled by Pulse Width Modulation with α duty cycle operating on the Boost structure (Fig 12). The constant frequency is *fd*=1/*Td* .With the PWM control this chopper is describe by the following average model.

$$\begin{cases} Vfc = L_1 \dfrac{dIL}{dt} + (1-\alpha)Vdc \\ IL(1-\alpha) = Cf \dfrac{dVdc}{dt} + Idc \end{cases} \qquad (16)$$

Where : *Vfc* is the Fuel Cell output Voltage

IL is the self current (output Fuel Cell current)

Vdc is the DC link voltage

Idc is the DC current delivered to the DC link

This chopper is voltage regulated to control the DC bus. To achieve accurate voltage regulation, two control loops have been realised, one on the current and the other one on the voltage [6]. Note that the inner current control loop is fast acting, while the outer voltage loop has a dynamic response that is a decade slower. Both loops use sampled polynomial RST controllers. The 'I_{bus}' parameter is considered as a disturbance that is both measured and compensated in the controller. A linear current model is first written, noting :

$$\alpha = \frac{VL' - Vfc}{Vdc} + 1 \qquad (17)$$

With this linearisation the current model is:

$$T_1(p) = \frac{Il(p)}{VL'(p)} = \frac{1}{L_1 p} \qquad (18)$$

To implement a digital controller we numerise the transfer function with the sampling frequency equal to the switch frequency.

$$H(z^{-1}) = \frac{B(z^{-1})}{A(z^{-1})} = \frac{Td}{L_1} \frac{z^{-1}}{(1-z^{-1})} \qquad (19)$$

Finally we established a classical sampled regulation structure (Fig. 13) with an RST (digital proportional and integrator controller):

$$S(z^{-1}) = 1 - z^{-1}; R(z^{-1}) = r_0 + r_1 z^{-1} \; T = R(1) \qquad (20)$$

This regulation coefficient are calculated by the pole placement. The characteristic polynomials of the closed loop is.

$$P(z^{-1}) = 1 + p_1 z^{-1} + p_2 \; z^{-2} = (1 - z^{-1} \exp(-\omega Td))^2 \qquad (21)$$

with: $\omega = 2\pi fd/10 = 3142\, rad/s$.

We obtain:

$$\begin{cases} r_0 = \frac{L_1}{Td}(p_1 + 2) \\ r_1 = \frac{L_1}{Td}(p_2 - 1) \end{cases} \quad (22)$$

Remark : In order to avoid wind-up we have implemented an anti-windup structure in the regulation loop to obtain the complete scheme presented in Figure 14.

In the same way, to add a voltage control loop, we realised a linearisation by an inverse model with:

$$Iref = \frac{Vdc}{Vfc}(Iref' + Idc) \quad (23)$$

So we can write the voltage model:

$$T_2(p) = \frac{Vdc(p)}{Iref'(p)} = \frac{1}{Cf\ p} \quad (24)$$

We have here the same type of transfer function than in the voltage loop so we made the same digital controller.

The structure of this controller is show in Fig 15.

The coefficient of the regulation are.

$$\begin{cases} r_0 = \frac{Cf}{Te}(p_1 + 2) \\ r_1 = \frac{Cf}{Te}(p_2 - 1) \end{cases} \quad (25)$$

Here we have the same characteristic polynomials with: $\omega = 2\pi fd/100 = 314\,rad/s$.

We have also implement the same type of anti-windup in the voltage loop (like in the current loop).

7.3- Buck/Boost Modelling and Control.

The chopper in Figure 16, is describe by the following average model which allows us to establish the equation in the two working phases [7].

Differentials equations in Buck case :

$$\frac{disc}{dt} = \frac{1}{L_2} Vdc\ \alpha_1 - \frac{Rsc}{L_2} isc - \frac{Vc}{L_2} \quad and \quad \frac{dVc}{dt} = \frac{isc}{Csc} \quad (26)$$

Differentials equations in Boost case :

$$\frac{disc}{dt} = \frac{1}{L_2} Vdc\ (1 - \alpha_2) - \frac{Rsc}{L_2} isc - \frac{Vc}{L_2} \quad and \quad \frac{dVc}{dt} = \frac{isc}{Csc} \quad (27)$$

In order to simulate this chopper we write:

$$Vpwm = \alpha_1 Vdc\ Buck/Boost + (1 - \alpha_2)\, Vdc\ \overline{Buck/Boost} \quad (28)$$

Where the 'Buck/Boost' variable is binary and represents the mode of operation for the chopper. The chopper is current regulated to manage the charge and discharge of the ESS [10]. In order to have one model and one regulator we note that the control in the boost mode is the complement of the control in the Buck mode. In this case the Boost model can be written as a Buck model and in the control loop we can compute the complement value of the cycle rate when the Boost operation is activated. The current transfer function is:

$$T(p) = \frac{Isc}{\alpha} = \frac{Csc\,Vdc\;p}{1 + Rsc\,Csc\;p + L_2\;Csc\;p^2} \qquad (29)$$

The DC link voltage is constant because this voltage is control by the Boost chopper.

To implement a digital controller we numerise the transfer function, the sampling frequency is equal to the switch frequency.

$$H(z^{-1}) = \frac{B(z^{-1})}{A(z^{-1})} = \frac{b_1 z^{-1}(1 - z^{-1})}{1 + a_1 z^{-1} + a_2 z^{-2}} \qquad (30)$$

We established a sampled regulation structure as on Figure 17. We computed an RST regulator with these polynomials:

$$S(z^{-1}) = 1 - z^{-1};\; R(z^{-1}) = r_0 + r_1 z^{-1}\;\; T = \frac{A(1) + b_1 R(1)}{b_1} \qquad (31)$$

The function in the *f*(*u*) bloc is the implemented function to calculate the complement value of the cycle rate when the Boost operation is activated. So we write:

$$alpha = u\;Buck\;/\;Boost + (1-u)\overline{Buck\;/\;Boost} \qquad (32)$$

The type of the chopper operation variable (Buck/Boost) is calculated by a relay shown in Figure 18. This is calculated by a relay because the zeros value of the current must be in the two modes because the chopper can make a current with a zero average value. So we have:

Buck mode when Buck/Boost=1.

Boost mode when Buck/Boost=0.

Note that when the current is near zero, the converter operates in the discontinuous conduction mode. One approach is to allow the switched model to operate in both boost and buck modes so that over a complete switching cycle the positive and negative current peaks cancel. A second preferred approach is to restrict the behaviour to one mode at a time and to add a filter on the current signal with a numerical Butterworth (4^{th} orders) filter $F(z^{-1})$. The regulation coefficient are calculates by the pole placement.

$$\begin{cases} r_0 = (p_1 - a_1)/b_1 \\ r_1 = (p_2 - a_2)/b_1 \end{cases} \qquad (33)$$

The characteristic polynomials is:

$$P(z^{-1}) = 1 + p_1 z^{-1} + p_2\;\; z^{-2} = (1 - z^{-1}\exp(-\omega Td))^2 \qquad (34)$$

Where: $\omega = \omega_{fil}/10 = 1500\,rad/s$ and ω_{fil} is the angular frequency cutting of the filter.

Because of current overshoot when the chopper operation changed, we must initialised the duty cycle at each changed to set the current to zero.

The initialised value is: $\alpha_{init} = Vsc/Vdc$

The implementation structure of the loop regulation with initialisation and anti-windup is given in Figure 19 scheme.

The initialisation is computed by the structure seen on Figure 20. The total structure presented in Figure 21, detects the mode modification and put the control variable to its initial value. The current reference is calculated in function of the ESS power reference and the losses estimation of the chopper. The power reference is calculated by an energy strategy.

In Buck case :

$$ESS\ power\ ref\,(k) = Power\ ref\,(k) + PLosses(k-1) \qquad (35)$$

In Boost case :

$$ESS\ power\ ref\,(k) = Power\ ref\,(k) + PLosses\,(k-1) \qquad (36)$$

The current reference is also managed by a logical function in order to limit the supercaps voltage (in max and min value). The losses of the chopper are estimated in average value by a value plant [8][9].

7.4- Simulation results.

The aim of these simulations (Figure 22 and 23) in average value is to view some responses of the main system variables. Data used for the power reference are taken from ADVISOR (NREL software) simulation and represents actual measurement on a train. We can see that the first converter has a voltage regulation and this voltage remains constant (150V) despite the power request on the DC link (see Fig 24). The simulation (Figure 23) shows also that the second chopper has a current regulation and the current in the supercaps tracks the current reference. We can also see that this chopper is bi-directionnal in current.

As we can see on Figure 24, the power of the Propulsion motor and auxiliaries is separated between the Fuel Cell and the supercaps following the basic energy management chosen. The quasi-static model seems to be sufficient for the power train simulation but, we are now testing if we must develop a dynamic model of the Fuel Cell.

8- Conclusion.

In order to control the Fuel Cell System we develop the Fuel Cell model, the air compressor model, and the valves model. We have only developed in this paper the control structure of the air supply system and pressure valves. But in the Fuel Cell System, there are other auxiliaries to control, like the cooling system to control the PEMFC temperature. So we must continue the study on the control structure [10].

In this paper a study of a Fuel Cell powered traction system has been realised in order to understand the dynamic behaviour of the system. This study has examined mainly the electrical characteristics of the converters in the system to determine the ability of the Fuel Cell to adequately supply the transient loads required. To this end, actual power load profiles from an existing traction application have been used in the simulations.

In the first section of the paper an electro-chemical model of the Fuel Cell itself has been presented. This provided a detailed dynamic model that can be combined with an electrical model of the remainder of the system (i.e. the provision of the required air and hydrogen mix at the correct pressure and flow rates to achieve the nominated cell operating point).

In the second part of the paper, the control structures for the electrical choppers on the power train have been presented and simulated, considering the properties needed for the Fuel Cell System and the Energy Storage System.

A voltage elevator Boost chopper structure have been designed and controlled in voltage to link the Fuel Cell System to the DC bus. Another Buck/Boost chopper is used to link the Energy Storage System to the same DC bus and controlled to manage the supercaps current.

Finally, we have build a global simulator on Matlab/Simulink in order to see if the voltage and current variables are controlled and if the control structures can realised the energy strategy management. Now, we can conclude that the voltage and the current in the power train are well controlled because the management of energy is realised and safety of Fuel Cell and supercaps are obtained.

Our future works are the control of a high power train with Fuel Cell with a global strategy management to control the power reference of each sub-system locally or globally on a known road/power profile. In this way we can have an optimal management which reduces the consumption or increases the global efficiency.

9- Appendix.

Fi	Molar flow of species i (O_2, H_2, N_2)
N	Number of cells by stack (586).
F	Faradays constant 96485 C/mol.
I	Current in A.
λ_{H_20}	Hydration rate of the membrane.
X_{0_2}	Molar fraction of 0_2 in air =21%
StO_2	Stochiometry rate of oxygen (1.6).
R	Molar gas constant. 8.13 J/K/mol.
V_{cath}	Cathodic Volume is 0.11 m^3
T_{fc}	Temperature in Kelvin (353.15°K).
Pi	Pressure in Pascal of gas i.
Cyl	Compressor capacity is 36.5 cm^3.
ω	Rotation speed in rad/s.
γ	Polytropic exponent, for air γ=1.4.
M	Molar masse of air.

10- References.

[1] W Friede, S Raël, B Davat: “PEM fuel cell models for supply of an electric load”, proceedings of Electrimacs 2002, August 18-19.

[2] Jay T.Pukrushpan, Anna G.Stefanopoulou, Huei Peng: “Modeling and Control for PEM Fuel Cell Stack System”, proceedings of the American Control Conference – Anchorage, Michigan - May 8-10-2002.

[3] VARAIX corporation documentation: “Compressor efficiency definitions” and “ Evaluation of vairex air system technology for automotive fuel cell power systems (fcps) “: website www.vairex.com

[4] Bird, Stewart, light foot: book: “Transport Phenomena" p481, Wiley international edition, ISBN: 0-471-07395-4

[5] Wiartalla Andreas, Lang Olivier, Pischinger Stefan, Schönfelder Carter: “Efficiency Boosting of Fuel Cell System Considering Part Load Operation”, proceedings of FISITA 2001 World Automotive Congress -Helsinki, Finland – June 2-7-2002

[6] M.Fadel :”Lois de commande pour une alimentation AC/DC à absorption de courant sinusoïdal”, proceedings of 3EI 2000.

[7] B.J.Arnet, L.P.Haines: “High Power DC-to-DC Converter For Supercapacitors”, proceedings of IEMDC 2001 – Boston, Massachusetts.

[8] International Rectifier documentation: “Application characterisation of IGBT’s” : website: www.irf.com/technical-info/an990/an-990.htm.

[9] EUPEC corporation data-sheet: “ EUPEC :FZ 1600 R 17 KF6 B2” : website www.eupec.com.

[10] J. Lachaize, M. Fadel, S. Caux, P. Schott and L. Nicod: "Modelling and control of a Fuel Cell in transport applications.", proceedings of IFAC 2003 - 15-19 september 2003 Seoul, Corea.

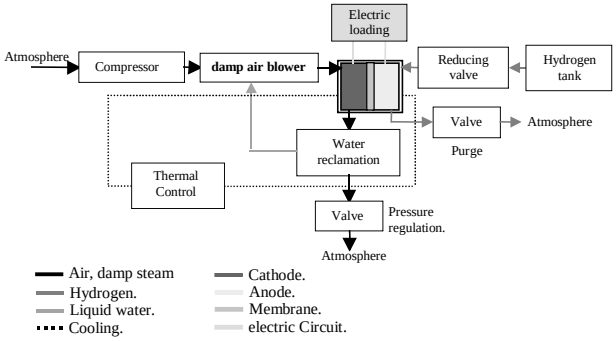

Fig 1. : Fuel Cell System.

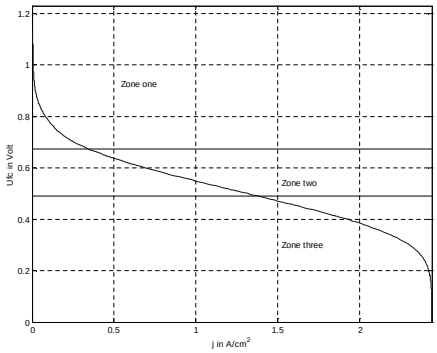

Fig 2. : Polarisation curve.

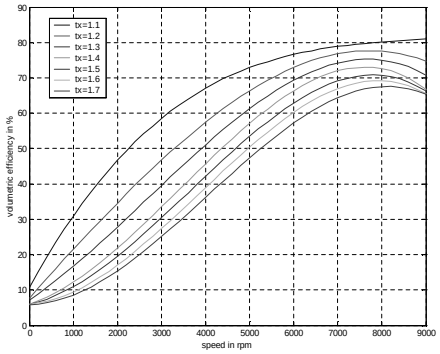

Fig 3. : Volumetric efficiency.

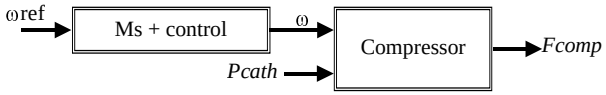

Fig 4. : Synchronous machine and compressor.

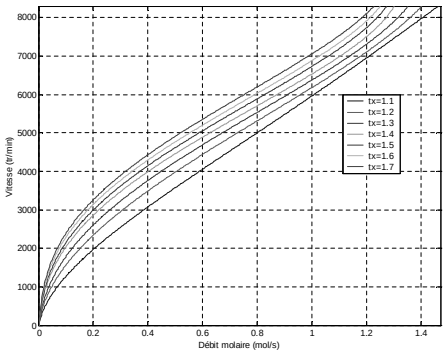

Fig 5. : compressor inverse model.

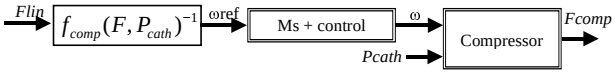

Fig 6. : flow modelling.

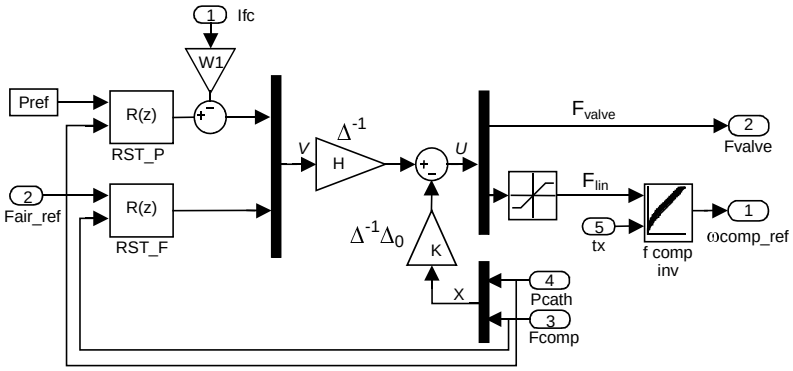

Fig 7. : Pressure and flow control.

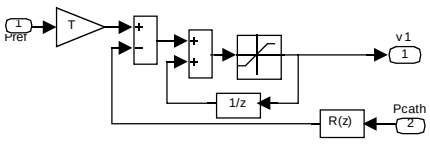

Fig 8. : Pressure and flow regulator.

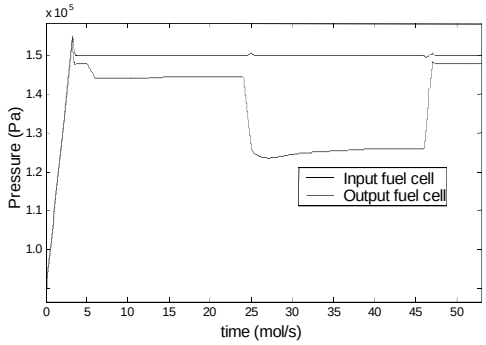

Fig 9. : Cathodic pressure.

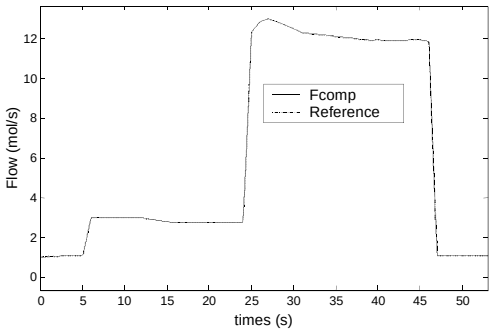

Fig 10. : Compressor flow

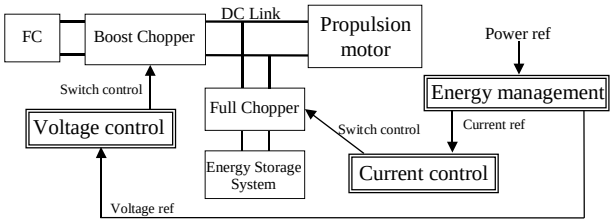

Fig 11. : Power Train and control structure.

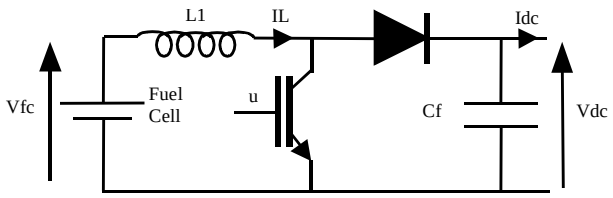

Fig 12. : Boost principle schema.

$\{L1 = 0.95mH \ and \ Cf = 3.2mF\}$

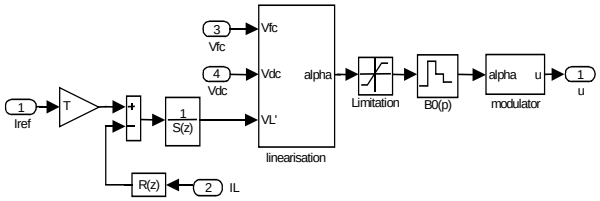

Fig 13. : Boost current loop.

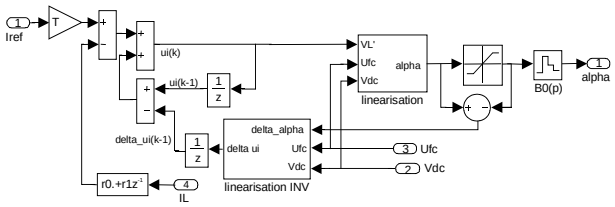

Fig 14. : Boost current loop implementation.

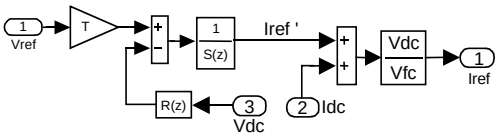

Fig 15. : Boost voltage loop.

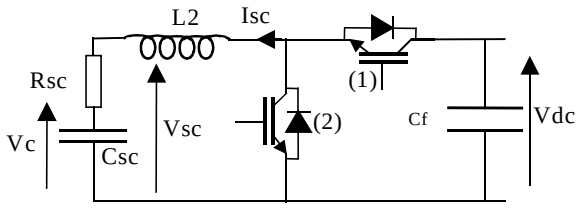

Fig 16. : Buck/Boost principle schema.

$$\{L2 = 0.94mH\,;Cf = 3.2mF\,;rsc = 55m\Omega\,;Csc = 47F\}$$

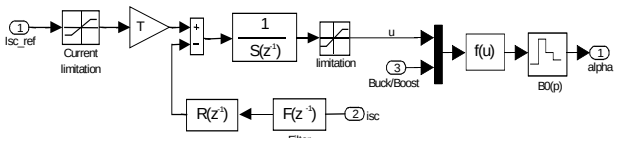

Fig 17. : Buck/Boost current loop.

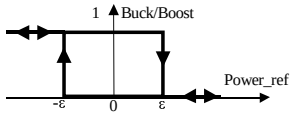

Fig 18. : Buck/Boost operation.

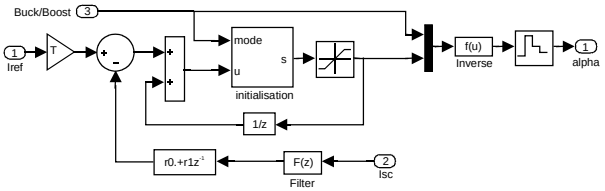

Fig 19. : Current regulation implementation.

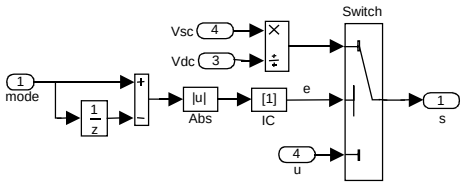

Fig 20. : Initialization computed.

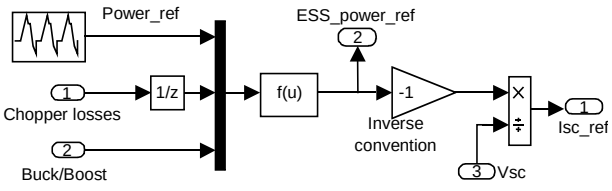

Fig 21. : Current reference.

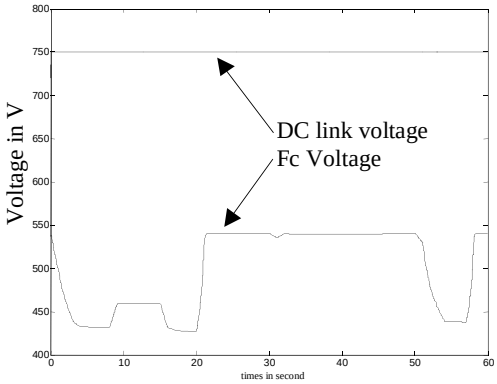

Fig 22. : DC link and FC voltage

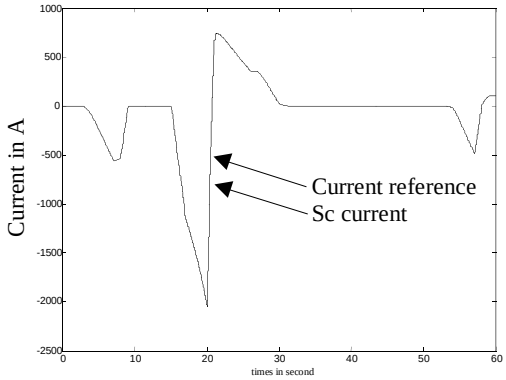

Fig 23. : Desired and real current

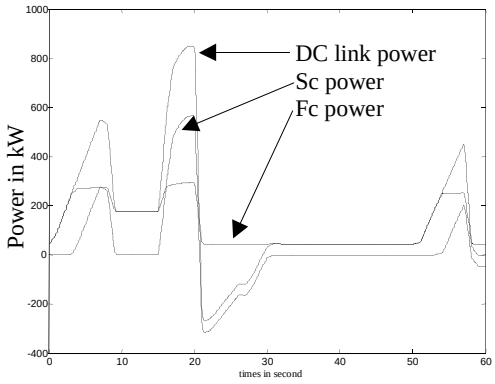

Fig 24. : power traction on an operating cycle.